Eawag_09525

Environmental Science & Technology

Article

pubs.acs.org/est

Substrate and Enzyme Specificity of the Kinetic Isotope Effects Associated with the Dioxygenation of Nitroaromatic Contaminants

Sarah G. Pati,[†,‡] Hans-Peter E. Kohler,[†] Anna Pabis,[¶,∥] Piotr Paneth,[¶] Rebecca E. Parales,[§] and Thomas B. Hofstetter*[,†,‡]

[†]Eawag, Swiss Federal Institute of Aquatic Science and Technology, 8600 Dübendorf, Switzerland

[‡]Institute of Biogeochemistry and Pollutant Dynamics (IBP), ETH Zürich, 8092 Zürich, Switzerland

[¶]Institute of Applied Radiation Chemistry, Lodz University of Technology, 90-924 Lodz, Poland

[§]Department of Microbiology and Molecular Genetics, University of California, Davis, California 95616, United States

Supporting Information

ABSTRACT: Compound-specific isotope analysis (CSIA) is a promising approach for tracking biotransformation of organic pollutants, but isotope fractionation associated with aromatic oxygenations is only poorly understood. We investigated the dioxygenation of a series of nitroaromatic compounds to the corresponding catechols by two enzymes, namely, nitrobenzene and 2-nitrotoluene dioxygenase (NBDO and 2NTDO) to elucidate the enzyme- and substrate-specificity of C and H isotope fractionation. While the apparent ^{13}C- and ^{2}H-kinetic isotope effects of nitrobenzene, nitrotoluene isomers, 2,6-dinitrotoluene, and naphthalene dioxygenation by NBDO varied considerably, the correlation of C and H isotope fractionation revealed a common mechanism for nitrobenzene and nitrotoluenes. Similar observations were made for the dioxygenation of these substrates by 2NTDO. Evaluation of reaction kinetics, isotope effects, and commitment-to-catalysis based on experiment and theory showed that rates of dioxygenation are determined by the enzymatic O_2 activation and aromatic C oxygenation. The contribution of enzymatic O_2 activation to the reaction rate varies for different nitroaromatic substrates of NBDO and 2NTDO. Because aromatic dioxygenation by nonheme iron dioxygenases is frequently the initial step of biodegradation, O_2 activation kinetics may also have been responsible for the minor isotope fractionation reported for the oxygenation of other aromatic contaminants.

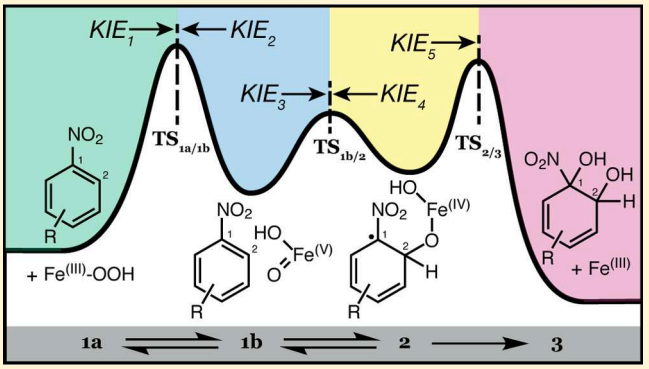

INTRODUCTION

Compound-specific stable isotope analysis of nitroaromatic contaminants has shown that all (bio)degradation routes investigated to date are associated with a measurable change of the substrate's C, H, or N isotope composition.[1−9] While reductive transformations of nitroaromatic compounds (NACs) are initiated by bond cleavage reactions at N−O bonds, oxidations involve the breaking of aromatic and aliphatic C−H bonds.[10,11] Consequently, systematic variations of stable C, H, and N isotope ratios in individual nitroaromatic soil and water contaminants allow one to distinguish reductions from mono- and dioxygenations of aromatic moieties as well as oxidations of methyl groups.[4−6] Such multielement isotope fractionation trends are typically stronger for (bio)transformation reactions than for nonreactive loss processes, such as sorption,[12] and we found that compound-specific isotope analysis (CSIA) enables the assessment of the various biodegradation routes of 2,4,6-trinitrotoluene (TNT) and its synthesis precursors (i.e., mono- and dinitrotoluenes) in contaminated soil.[5]

Enzymatic oxygenations of aromatic rings of NACs are typically associated only with minor C and H isotope fractionation. Similar observations were made for other aromatic contaminants, such as alkylated and chlorinated benzenes and naphthalene.[13−17] Apparent kinetic isotope effects (AKIEs) for dioxygenations, which are calculated for the reactive position of a compound from its isotope fractionation,[18] can indeed differ significantly. For example, the ^{13}C-AKIEs for dioxygenation of NACs vary between 1.004 and 1.024 and overlap with values reported for all other biodegradation reactions of NACs including ring monooxygenation (1.002 to 1.011).[4,6,19,20] Variations of isotope fractionation were found for different substrates transformed by the same enzyme and *vice versa*, that is for the same substrate transformed by different enzymes. It is apparently difficult to

Special Issue: Jerry Schnoor's Lasting Influence on Global and Regional Environmental Research

Received: October 16, 2015
Revised: February 18, 2016
Accepted: February 19, 2016
Published: February 19, 2016

DOI: 10.1021/acs.est.5b05084
Environ. Sci. Technol. 2016, 50, 6708−6716

delineate a "typical" magnitude of isotope fractionation for (bio)degradation routes initiated by oxidations of aromatic moieties unless the substrate and enzyme specificities of AKIEs are understood better.

Investigations of nitroarene dioxygenases have indeed shown that small differences in the active site, such as an exchanged amino acid residue, can have a strong impact on substrate specificity, regiospecificity, and enantioselectivity of the enzyme.[21,22] For example, 95% of the amino acid residues within the subunit containing the active site are identical in nitrobenzene dioxygenase (NBDO) from *Comamonas* sp. strain JS765 and 2-nitrotoluene dioxygenase (2NTDO) from *Acidovorax* sp. strain JS42.[21,23] Nevertheless, NBDO and 2NTDO have different regiospecificities and enantioselectivities toward some nitroaromatic substrates. For instance, 3-nitrotoluene is transformed exclusively to 4-methylcatechol by NBDO while with 2NTDO the transformation of 3-nitrotoluene results in a mixture of 3-methylcatechol, 4-methylcatechol, and 3-nitrobenzyl alcohol.[21,22] It was hypothesized that these different substrate specificities are largely caused by only one different amino acid residue in the active site, which is a phenylalanine in NBDO and an isoleucine in 2NTDO.[24,25] It is well-known that enzyme−substrate interactions, such as the ones exemplified above, can alter the rate-limiting steps of biotransformation reactions and, consequently, the associated isotope effects.[26−29] For nitroarene dioxygenations, potentially rate-limiting steps include substrate binding, activation of molecular O_2, and the subsequent, isotope sensitive hydroxylation of the aromatic moiety. However, in contrast to many well-studied biochemical reactions, the consequences of specific enzyme−substrate interactions on the observable isotope fractionation of enzymatic transformations of organic contaminants are not well understood.

The goal of this work was to explore reactions of nitroarene dioxygenases with a series of substrates for systematic changes of the observable C and H isotope fractionation and variations of the corresponding ^{13}C- and ^{2}H-AKIEs. To this end, we performed incubations of six different substrates (i.e, nitrobenzene, 2-, 3-, and 4-nitrotoluene, 2,6-dinitrotoluene, and naphthalene) with whole cells of *E. coli* clones expressing NBDO or 2NTDO and enzyme assays with purified NBDO. C and H isotope fractionation were determined for each substrate, and the ^{13}C-AKIEs of dioxygenation were derived from the combined substrate and product C isotope fractionation obtained from isotopic analysis by GC/IRMS and LC/IRMS.[20] Measured C and H isotope fractionation was benchmarked against theoretical ^{13}C- and ^{2}H-KIEs (i) to identify the rate-limiting steps of nitrobenzene dioxygenation by NBDO and (ii) to elucidate the origins of the observed substrate-specific isotope fractionation.

EXPERIMENTAL SECTION

All chemicals used in this study are reported in Section S1.

Experiments with *E. coli* Clones Expressing NBDO or 2NTDO. Two *Escherichia coli* strains were used in this study, *E. coli* VJS415(pK19::927)[30] with the *nbzAaAbAcAd* genes from *Comamonas* sp. strain JS765[21] and *E. coli* DH5α-(pDTG800),[23] which carries the *ntdAaAbAcAd* genes from *Acidovorax* sp. strain JS42.[31,32] Both strains were grown in LB (5 g L^{-1} yeast extract, 10 g L^{-1} tryptone, 5 g L^{-1} NaCl) at constant temperatures (30 or 37 °C) with shaking. LB solutions were supplied with 100 mg L^{-1} kanamycin sulfate and 200 mg L^{-1} sodium ampicillin for *E. coli* VJS415(pK19::927) and *E. coli* DH5α(pDTG800), respectively. Cells were harvested at late log-phase (OD_{600} between 3 and 4) by centrifugation at 20 000*g* for 20 min, washed, and resuspended in phosphate buffer (40 mM KH_2PO_4, pH 7.0) to final cell dry weights of 3−9 g L^{-1}.

Degradation experiments with whole cells of *E. coli* clones were performed in duplicate. Cell suspensions of 200 mL were incubated at 30 °C with shaking (220 rpm) in 240 mL serum flasks sealed with Viton rubber stoppers. To initiate transformation reactions, aliquots of a methanolic stock solution (0.1 to 1.0 mL) containing nitrobenzene or a nitrotoluene isomer were added resulting in appropriate initial substrate concentrations (0.5 or 1.0 mM). At predefined timepoints, samples were withdrawn with a glass syringe and cells were removed by centrifugation. Supernatants were stored at 4 °C until chemical analysis. For measurement of product isotope fractionation, experiments were repeated under identical conditions using smaller volumes (20 mL cell suspension in 25 mL flasks) and samples were analyzed immediately by LC-IRMS.

Experiments with Purified NBDO. We studied the dioxygenation of 2,6-dinitrotoluene and naphthalene by NBDO with purified NBDO components to minimize sorption losses and reductive side-reactions. Previous work[20] has shown that isotope fractionation during dioxygenation of nitroaromatic compounds by NBDO in experiments with *E. coli* clones and purified enzymes lead to identical results. The three enzyme components of NBDO were purified using methods[20] adapted from Parales et al.[33] Purified oxygenase, ferredoxin, and reductase were mixed in MES buffer (50 mM, pH 6.8) containing 0.1 mM $(NH_4)_2Fe(SO_4)_2$ at concentrations of 0.3 μM, 3.6 μM, and 0.3 μM, respectively.[21,33] 2,6-Dinitrotoluene (100 mM in methanol) or naphthalene (20 mM in 3:7 ethanol:water) was added to give initial concentrations of 100 μM to reactors containing 5 mL of buffered enzyme solution. To achieve variable extents of substrate conversion, different amounts of 0.1 M NADH (in 0.01 M NaOH, final concentration of 0−500 μM) were added to separate reactors. Reactors were incubated at 30 °C with shaking (100 rpm) for 30 min before chemical analysis.

Chemical and Isotopic Analyses. Methods for quantifying substrates and products were used as described previously.[20] Briefly, concentrations of NACs and aromatic products were determined by reversed-phase HPLC coupled to a UV−vis detector. Compounds were separated on appropriate C18-columns (see Section S2 for details). Nitrite was quantified using a photometric method[34] at 540 nm with the reagents sulfanilamide (10 g L^{-1} in 1.5 M HCl) and *N*-(1-naphthyl)-ethylene diamine (1 g L^{-1} in 1.5 M HCl).

Carbon and hydrogen isotope ratios (δ^{13}C and δ^{2}H) of all nitroaromatic substrates and naphthalene were measured by isotope ratio mass spectrometry after solid-phase microextraction (65 μm of PDMS/DVB or 85 μm of polyacrylate coating, Supelco) and gas chromatography as reported previously.[35−37] Aqueous samples were filtered and diluted to concentrations corresponding to constant peak amplitudes. Depending on the compound and element, peak amplitudes were between 0.6 and 8 V. Isotope ratios are reported as arithmetic means of triplicate measurements in the form of isotope signatures (δ^{13}C and δ^{2}H) in per mil (‰) relative to the international reference materials Vienna PeeDee Belemnite ($\delta^{13}C_{VPDB}$) and Vienna Standard Mean Ocean Water ($\delta^{2}H_{VSMOW}$). We used a suite of calibrated reference materials

DOI: 10.1021/acs.est.5b05084
Environ. Sci. Technol. 2016, 50, 6708−6716

Scheme 1. Proposed Mechanism of Nitrobenzene Dioxygenation by NBDO[45] with Rate Constants of Elementary Reaction Steps k_1 through k_5[a]

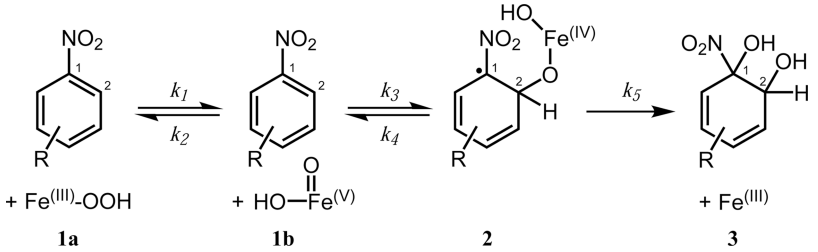

[a]Initial O−O bond cleavage in the Fe(III)-hydroperoxide complex (**1a**) results in an Fe(V)-oxo-hydroxide complex (**1b**) that reacts with the nitroaromatic substrate in a step-wise dioxygenation. The first C−O bond formation step occurs at the C-2 atom of the substrate and results in a radical intermediate (**2**) that undergoes a second C−O bond formation at the C-1 atom to yield the *cis*-dihydrodiol product.

with $\delta^{13}C$ from −54.6‰ to 7.7‰ and $\delta^{2}H$ from −118‰ to 506‰[38,39] as well as repeated measurements of in-house standards (NACs of known C isotope signatures) in a standard bracketing procedure to ensure accuracy of the measured $\delta^{13}C$- and $\delta^{2}H$-values.

$\delta^{13}C$ analysis of 3-methylcatechol, 4-methylcatechol, and 4-nitrobenzyl alcohol was carried out by liquid chromatography/isotope ratio mass spectrometry (LC/IRMS)[40,41] using a Dionex UltiMate 3000 system coupled to a Finnigan LC IsoLink and a Delta V Plus IRMS (Thermo Scientific). As described previously,[20] three to six injections were made from the same, cooled vial with adjusted injection volumes of samples and standards to give constant peak amplitudes between 0.7 and 4 V. An eluent of 100% phosphate buffer (10 mM KH_2PO_4, pH 2.5) was used at 0.5 mL min^{-1} with an XBridge C18 column (2.5 μm, 3 × 50 mm, Waters) in a high-temperature HPLC 200 column oven (Scientific Instrument Manufacturer).

Computational Methods. Position-specific ^{13}C- and ^{2}H-KIEs for nitrobenzene dioxygenation by NBDO were calculated with a hybrid quantum mechanical/molecular mechanical (QM/MM) approach. Calculations were performed with the *f*Dynamo library[42] and the Gaussian 09[43] electronic structure package. The dioxygenation of nitrobenzene was modeled in a heterohexameric model of NBDO, which was obtained from the molecular dynamics simulation in an aqueous environment[44] and additionally soaked in a 165 × 165 × 165 $Å^3$ water box. The system was divided into a QM and MM region.[45] The QM subsystem, which contained nitrobenzene, the iron-dioxygen complex, and the side chains His211, His206, Asp360, Asn258, Asn199, Asn295, and Asp203, was treated at the DFT level with the hybrid B3LYP functional.[46,47] The 6-31G* basis set was used for C, H, N, and O atoms and combined with the Hay and Wadt effective core potential (ECP)[48] for the description of the Fe atom. The remainder of the protein constituted the MM subsystem and was described using the OPLS-AA force field, which was combined with the previously employed Amber parameters for the treatment of the metal centers in the system.[44] The iron-dioxygen complex was modeled in the sextet state (S = 5/2) as a positively charged protonated species, i.e., $[Fe^{III}-OOH]^{2+}$ or $[HO-Fe^{V}=O]^{2+}$. Solvent molecules were described with the TIP3P flexible potential. The coordinates of all atoms beyond 20 Å from the mononuclear iron center in the QM region were fixed.

With the above model, transition states corresponding to the reaction steps presented in Scheme 1 were optimized. The product and reactant states were traced from each transition state by following an intrinsic reaction coordinate (IRC) algorithm and optimized subsequently. The nature of all stationary points was verified by performing vibrational frequency calculations. Optimized structures of the stationary points along the reaction were then used to calculate semiclassical isotope effects. Position-specific ^{13}C- and ^{2}H-KIEs were obtained from the total partition functions and zero point energies calculated for the two isotopologs with a light or heavy atom at a given C or H position in the transition state and the reactant. KIEs were obtained separately for all C and H atoms of nitrobenzene from 8 different configurations of the enzyme that were taken from the last 2 ns of the MD simulation of NBDO published earlier.[44] The position-specific KIEs are reported as average values of these 8 calculations in Table S2 and referred to as *theoretical* KIEs.

Data Evaluation. Bulk isotope enrichment factors (ϵ_E) were obtained from a linear regression of substrate C and H isotope signatures ($\delta^{13}C$, $\delta^{2}H$) vs the fraction of the remaining substrate (c/c_0) according to eq 1.

$$\ln\left(\frac{\delta^{h}E + 1}{\delta^{h}E_0 + 1}\right) = \epsilon_E \cdot \ln(c/c_0) \quad (1)$$

where $\delta^{h}E_0$ and $\delta^{h}E$ are the initial isotope signature of element E and the value measured during the reaction, respectively. Data from replicate experiments were combined using the Pitman estimator.[49] A linear regression was applied to measured H and C isotope signatures ($\delta^{2}H$ vs $\delta^{13}C$). The resulting regression slopes were used to compare two-dimensional isotope fractionation trends between nitrotoluene isomers. The slope from this linear regression ($\Lambda_{H/C}$) corresponds approximately to the ratio of bulk isotope enrichment factors (ϵ_H/ϵ_C).

Reaction-specific C isotope enrichment factors (ϵ^{j}_{C}) for dioxygenation and CH_3-group oxidation were derived on the basis of a set of differential equations as shown recently.[20] Concentrations and $\delta^{13}C$ of NACs and their organic oxidation products were fit with eq 2 implemented in Aquasim.[50]

$$\frac{dc_\kappa}{dt} = \sum_j \nu \cdot k_j \cdot c_\kappa \quad (2)$$

where c_κ is the concentration of each substrate and product C isotopologue, ν is a stoichiometric coefficient, and k_j is the rate of product formation from reaction j for each C isotopologue. ϵ^{j}_{C} was calculated from the ratio of product formation rate constants as demonstrated in eq 3. Additional evaluation of product C isotope fractionation is given in Section S3.

DOI: 10.1021/acs.est.5b05084
Environ. Sci. Technol. 2016, 50, 6708−6716

$$\epsilon_C^j = \frac{^{13}C k_j}{^{12}C k_j} - 1 \quad (3)$$

In experiments where only dioxygenation occurred, ^{13}C- and ^{2}H-AKIEs were derived from ϵ_E-values with eq 4, on the basis of the assumptions for the reaction mechanism.[18]

$$AKIE_E \approx \frac{1}{1 + n/x \cdot z \cdot \epsilon_E} \quad (4)$$

where n is the number of atoms of element E (C or H), x is the number of these atoms at the reactive position, and z is a correction for intramolecular isotopic competition. In experiments with side reactions, only ^{13}C-AKIEs could be derived by substituting ϵ_E with ϵ_C^j for dioxygenation. For ^{13}C-AKIE, x and z were 2 whereas for ^{2}H-AKIE x and z were 1.

Experimental AKIEs derived with eq 4 and theoretical KIEs were used for two purposes. (i) With position-specific KIEs from Table S2, we derived theoretical C and H isotope enrichment factors, ϵ_C^* and ϵ_H^*, as well as $\delta^{13}C$ vs $\delta^{2}H$-correlation slopes, $\Lambda_{H/C}^*$, (see Eqs S17−S21) with the assumption that only one of the 3 elementary reaction steps of the dioxygenation (i.e., O_2 activation and two C−O bond formation steps; see below) is limiting the rate of substrate transformation. To this end, eq 5 for AKIEs of multistep reaction was simplified for 3 scenarios as detailed in Section S6. (ii) We calculated the commitment factors (k_5/k_4 and $(k_3/k_2)(k_5/k_4)$) from eq 5 from a comparison of theoretical KIEs with experimental AKIE-values to obtain insights into the relative barrier heights of the transition states of the 3 reaction steps.[27,28]

$$AKIE = \frac{EIE_1EIE_3KIE_5 + EIE_1KIE_3(k_5/k_4) + KIE_1(k_3/k_2)(k_5/k_4)}{1 + (k_5/k_4) + (k_3/k_2)(k_5/k_4)} \quad (5)$$

where KIE_n and EIE_n are the theoretical kinetic and equilibrium isotope effects of the multistep reaction discussed below. Eq 5 for C and H isotopes was solved for the two commitment factors, which are identical for both elements. Finally, k_5/k_4 and $(k_3/k_2)(k_5/k_4)$ were interpreted in terms of differences of the Gibbs free energies, $\Delta\Delta G$, between transition states as shown in Section S7 (eqs S22−S23).

RESULTS AND DISCUSSION

Isotope Fractionation during Dioxygenation by NBDO: 4-Nitrotoluene. Our approach for the study of isotope effects associated with nitroarene dioxygenations is exemplified here in detail for the transformation of 4-nitrotoluene by NBDO, while we present the results for other substrates in more aggregated form in the following section. Figure 1a shows the disappearance of 4-nitrotoluene within 3.3 h during incubation with *E. coli* clones expressing NBDO (7.9 g L^{-1}). The dioxygenation products 4-methylcatechol and nitrite were produced in equal amounts during the entire experiment and accounted for 85% of 4-nitrotoluene losses (Figure 1a). Oxidation of the methyl group leading to 4-nitrobenzyl alcohol contributed to 8% to the disappearance of 4-nitrotoluene. Additional losses of up to 10% can be explained by sorption of the substrate to cells, which was observed to the same extent in previous work with comparable cell densities.[20]

The carbon isotope signatures, $\delta^{13}C$, of 4-nitrotoluene increased during the transformation of 4-nitrotoluene by NBDO (Figure 1b) indicating a preferential dioxygenation of

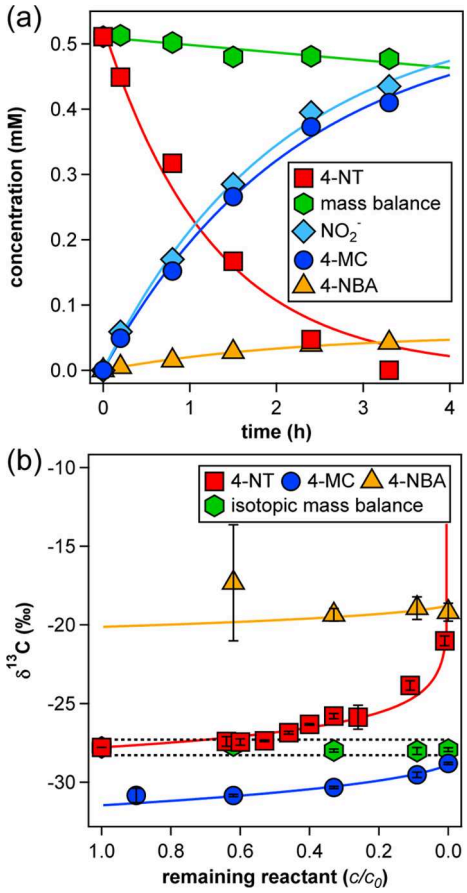

Figure 1. (a) Concentrations and (b) carbon isotope signatures of 4-nitrotoluene (4-NT, red squares), 4-methylcatechol (4-MC, dark blue circles), 4-nitrobenzyl alcohol (4-NBA, yellow triangles), and nitrite (NO_2^-, light blue diamonds) in an experiment with *E. coli* clones expressing NBDO. Mass balances (green hexagons) represent the sum of concentrations or isotope signatures (weighted by concentrations) of the three organic compounds. Solid lines show pseudo-first-order kinetics or nonlinear regressions of eq 1 (4-nitrotoluene) and eq S1 (products). Dashed lines show the ±0.5‰ interval around the initial substrate isotope signature. Error bars represent standard deviations of triplicate measurements.

^{12}C isotopologues and accumulation of ^{13}C in the remaining substrate. This trend is reflected in the $\delta^{13}C$-values of the dioxygenation product 4-methylcatechol, which is depleted in ^{13}C isotopologues at an early stage of the reaction. At the end of the reaction, the $\delta^{13}C$ of 4-methylcatechol (−28.8 ± 0.1‰) was below the initial $\delta^{13}C$ of 4-nitrotoluene (−27.8 ± 0.1‰). This small mismatch is consistent with the fact that the C isotopes of 4-nitrotoluene end up not only in 4-methylcatechol but also to a minor extent in 4-nitrobenzyl alcohol (<9%). While $\delta^{13}C$-values of 4-methylcatechol are more negative than those of the substrate, $\delta^{13}C$-values of 4-nitrobenzyl alcohol are more positive. The excellent C isotope mass balance shown in Figure 1b implies that the two reactions (dioxygenation and methyl group oxidation) were the only isotope fractionating processes in our experimental system.

The bulk C isotope enrichment factor of 4-nitrotoluene (ϵ_C) amounted to −1.4 ± 0.4‰. The one for the dioxygenation reaction (ϵ_C^{diox}) can not be determined from $\delta^{13}C$-values of 4-methylcatechol without implicit assumptions for the isotope fractionation of the reaction leading to 4-nitrobenzyl alcohol. The much more positive $\delta^{13}C$-values for 4-nitrobenzyl alcohol

DOI: 10.1021/acs.est.5b05084
Environ. Sci. Technol. 2016, 50, 6708−6716

Table 1. Bulk Isotope Enrichment Factors (ϵ_C, ϵ_H), $\Lambda_{H/C}$-Values, γ_{diox}, Dioxygenation-Specific Isotope Enrichment Factors (ϵ_C^{diox}), ^{13}C- and ^{2}H-AKIEs for the Dioxygenation of Different (Nitroaromatic) Substrates by NBDO and 2NTDO[a]

entry	substrate	ϵ_C (‰)	ϵ_H (‰)	$\Lambda_{H/C}$ (−)	γ_{diox}[b] (−)	ϵ_C^{diox} (‰)	^{13}C-AKIE (−)	^{2}H-AKIE (−)
			Nitrobenzene Dioxygenase (NBDO)					
1	nitrobenzene	−3.7 ± 0.2[c]	−5.6 ± 1.2[c]	1.7 ± 0.5[c]	1.00	−4.1 ± 0.2[c]	1.025 ± 0.001[c]	1.027 ± 0.008[c]
2	2-nitrotoluene	−1.3 ± 0.1[c]	−4.6 ± 2.0[c]	2.8 ± 1.2[c]	0.55	−2.5 ± 0.2[c]	1.018 ± 0.001[c]	
3	3-nitrotoluene	−0.4 ± 0.2	−2.6 ± 1.6	1.5 ± 2.2	1.00	−1.4 ± 0.1	1.010 ± 0.001	1.019 ± 0.012
4	4-nitrotoluene	−1.4 ± 0.4	−5.5 ± 2.3	2.1 ± 0.6	0.91	[d]	1.010 ± 0.002[e]	
5	2,6-dinitrotoluene	−1.1 ± 0.4	−20 ± 4	15 ± 4	1.00		1.008 ± 0.003	1.128 ± 0.029
6	naphthalene	−0.4 ± 0.3	−15 ± 1	40 ± 28[f]	[g]		1.004 ± 0.001	1.120 ± 0.007
			2-Nitrotoluene Dioxygenase (2NTDO)					
7	nitrobenzene	−0.8 ± 0.2	−3.4 ± 1.2	3.4 ± 0.9	1.00		1.005 ± 0.001	1.017 ± 0.006
8	2-nitrotoluene	−0.4 ± 0.1	−3.5 ± 0.6	6.5 ± 1.5	0.93	−0.6 ± 0.1	1.004 ± 0.001	
9	3-nitrotoluene	−0.6 ± 0.2	−5.9 ± 0.7	6.9 ± 1.5	0.96[h]		1.004 ± 0.001[e]	
10	4-nitrotoluene	−0.1 ± 0.1	−2.6 ± 1.1	1.3 ± 3.9	1.00[i]	−0.4 ± 0.1	1.003 ± 0.001	

[a]Uncertainties correspond to 95%-confidence intervals. [b]Relative amount of dioxygenation products compared to the sum of dioxygenation and methyl group oxidation products. [c]Data from Pati et al.[20] [d]Not determined (see Section S6 for details). [e]Calculated from substrate isotope fractionation (ϵ_C). [f]Calculated as ϵ_H/ϵ_C. [g]No product standard available. [h]Combined contribution of 3-methylcatechol (66%) and 4-methylcatechol (30%). [i]Combined contribution of 4-methylcatechol (50%) and 2-methyl-5-nitrophenol (50%).

imply the formation of a common intermediate for both dioxygenation and methyl group oxidation. This finding is puzzling and difficult to reconcile with the fact that, in nonheme Fe dioxygenases, reactive oxygen species and aromatic substrates are bound in a way that is very specific for the catalyzed reaction[51−53] (see Section S5 for details and Elsner et al.[54] regarding data evaluation). The ϵ_C-value for dioxygenation is approximately 10‰ more negative than the one for methyl group oxidation. The small share of methyl group oxidation, however, makes this quantification very uncertain, and we refrain from quantifying ϵ_C^{diox} for 4-nitrotoluene.

Isotope Fractionation during Dioxygenation of Different Substrates by NBDO. We examined the C and H isotope fractionation of the reactions of 6 different substrates with NBDO, namely 2-, 3-, and 4-nitrotoluene, 2,6-dinitrotoluene, naphthalene, and nitrobenzene. The results are summarized in Table 1. Data for the transformation of 2-nitrotoluene and nitrobenzene by NBDO were taken from previous work.[20] Nitrobenzene, 3-nitrotoluene, and 2,6-dinitrotoluene exclusively underwent a dioxygenation reaction as quantified by the reaction products NO_2^- and the corresponding substituted catechols (Figures S5−S6). Naphthalene also reacted through dioxygenation as shown by Lessner et al.;[21] however, no product analysis was carried out due to the lack of standard material. Substituted nitrobenzyl alcohols, which are indicative for methyl group oxidations, were found only in experiments with 2- and 4-nitrotoluene as substrates.

We found very different C and H isotope enrichment factors (ϵ_C and ϵ_H, Table 1) for the disappearance of the various substrates. While ϵ_C for nitrobenzene was moderately large (−3.7 ± 0.2‰), the ϵ_C-value for 3-nitrotoluene was almost negligible and difficult to quantify (−0.4 ± 0.2‰). C isotope enrichment factors for the *dioxygenation* of NACs, ϵ_C^{diox}, which were determined from the $\delta^{13}C$ of the corresponding catechols, also varied considerably from −1.4 ± 0.1‰ to −4.1 ± 0.2‰ (Table 1, entries 1 and 3). Despite these noticeable substrate-specificities, the correlation of C and H isotope signatures ($\delta^{13}C$ vs $\delta^{2}H$) and the corresponding correlation slopes ($\Lambda_{H/C}$) suggest a common reaction mechanisms for the transformation of the three nitrotoluene isomers. As shown in Figure 2a, $\Lambda_{H/C}$-values were identical, despite the fact that the relative proportion of substrate undergoing dioxygenation, γ_{diox}, was different. In fact, γ_{diox} was large for 3- and 4-nitrotoluene (i.e., 1.00 and 0.91, Table 1, entries 3 and 4), and thus, dioxygenation can be expected to have dominated the correlation between H and C isotope fractionation. Methyl group oxidation of 2-nitrotoluene, which happens to the same extent as dioxygenation, was not subject to significant C and H isotope fractionation[20] (see Section S5 for current assumptions regarding data evaluation). Thus, even though there is good evidence for dioxygenation to be responsible for nitrotoluene isotope fractionations, ϵ_C^{diox}-values were distinctly different for each nitrotoluene isomer. As will be discussed further below, we hypothesize that this phenomenon originated from contributions of isotope insensitive but partially rate-limiting reaction steps preceding dioxygenation.

A rigorous quantitative comparison of $\Lambda_{H/C}$-values for nitrotoluenes with those for nitrobenzene, 2,6-dinitrotoluene, and naphthalene was hampered by the different number of C and H atoms of the substrates, although the differences in the number of C and H atoms between nitrobenzene and nitrotoluenes are small. Nitrobenzene contains less H (5 vs 7) and less C atoms (6 vs 7) than nitrotoluene so that $\Lambda_{H/C}$ for nitrobenzene should be larger (20%) than for nitrotoluene if the mechanisms, and thus intrinsic KIEs of dioxygenation, were identical. Our experiments show that the $\Lambda_{H/C}$ for nitrobenzene (1.7 ± 0.5) was within the expected range for a common rate-limiting reaction step during transformation of nitrobenzene and nitrotoluenes. In fact, $\Lambda_{H/C}$ for nitrobenzene was identical within experimental uncertainty of $\Lambda_{H/C}$ of the three nitrotoluenes (between 1.5 ± 2.2 and 2.8 ± 1.2, Table 1). Note that the large uncertainty of $\Lambda_{H/C}$ for 3-nitrotoluene originated from the small extent of C and H isotope fractionation. $\Lambda_{H/C}$-values for 2,6-dinitrotoluene and naphthalene were 15 ± 4 and 40 ± 28, respectively, and thus much larger than what could be explained with the differences of the number of H and C atoms alone. Therefore, correlations of C and H isotope fractionation for the dioxygenation of the six substrates by NBDO imply dioxygenation by at least two different reaction pathways, that is one for nitrobenzene and nitrotoluene isomers and another one for 2,6-dinitrotoluene and naphthalene.

Kinetic Isotope Effects and Mechanism of Nitroarene Dioxygenation by NBDO. Different reaction mechanisms

DOI: 10.1021/acs.est.5b05084
Environ. Sci. Technol. 2016, 50, 6708−6716

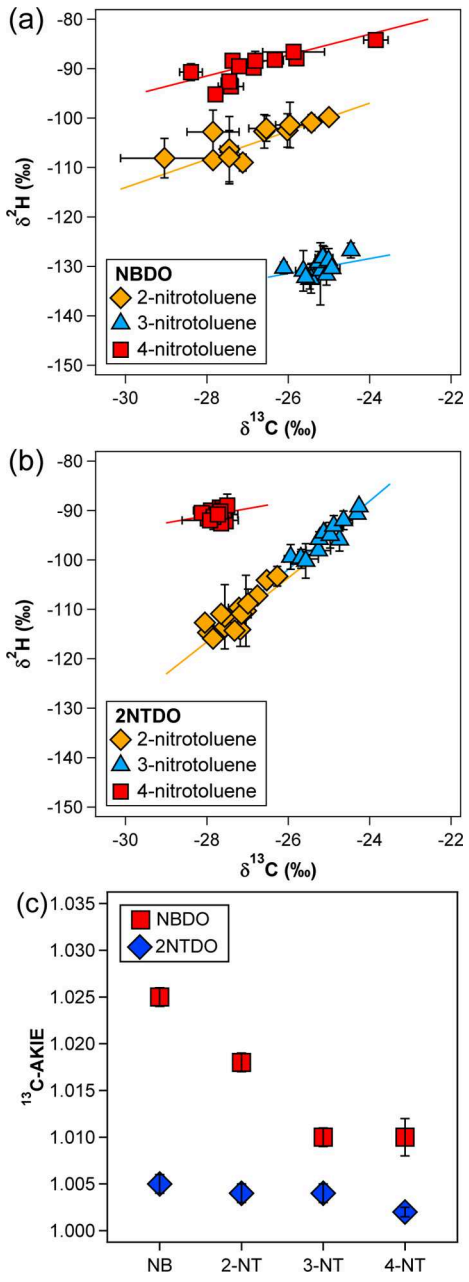

Figure 2. Two dimensional isotope fractionation (δ^2H vs δ^{13}C) for transformations of 2-nitrotoluene (yellow diamonds), 3-nitrotoluene (blue triangles), and 4-nitrotoluene (red squares) by NBDO (a) and 2NTDO (b). Solid lines represent linear regressions which have slopes that equal $\Lambda_{H/C}$. (c) ^{13}C-AKIE-values calculated for the dioxygenation of all nitroaromatic substrates with NBDO (red squares) and 2NTDO (blue diamonds). Error bars represent 95%-confidence intervals.

have indeed been proposed for the dioxygenation of aromatic compounds. In principle, dioxygenations can occur through concerted or stepwise hydroxylation of two aromatic C atoms by Fe(III)-hydroperoxide and Fe(V)-oxo-hydroxide species.[55,56] Computational evidence for nitrobenzene dioxygenation by NBDO suggests that the pathway shown in Scheme 1 is energetically most favorable.[45] Binding of the substrate is a prerequisite for activation of O_2 in nonheme Fe oxygenases.[51,57] Therefore, binding of nitrobenzene occurs before formation of an Fe(III)-hydroperoxide species (**1a**, Scheme 1) in the active site of NBDO. Cleavage of the O−O bond in **1a** results in an Fe(V)-oxo-hydroxide complex (**1b**). The latter reacts with the nitroaromatic substrate in a stepwise manner so that two C−O bonds are formed in two subsequent steps. The first C−O bond formation step occurs at the C-2 atom and results in a radical intermediate (**2**), which undergoes a second C−O bond formation at C-1 to yield a *cis*-dihydrodiol (**3**). NO_2^- is eliminated spontaneously from **3**, and catechol is the first organic product detectable during the dioxygenation reaction (not shown in Scheme 1).

We have calculated the position-specific ^{13}C- and ^{2}H-KIEs of nitrobenzene (Table S2) for the forward and backward reactions shown in Scheme 1 to identify rate-limiting reaction step(s) as well as the origin of the observed C and H isotope fractionation. In Table 2, we compiled *theoretical* values for

Table 2. ^{13}C- and ^{2}H-KIE*-Values for Reactive Positions (C-1, C-2, H-1) and ϵ*- and $\Lambda^*_{H/C}$-Values Calculated from Theoretical Position-Specific KIEs of Nitrobenzene Dioxygenation by NBDO in Table S2 Assuming That One of the Three Steps in Scheme 1 Is Exclusively Rate-Limiting

	rate-limiting step		
parameter	**1a** $\xrightarrow{k_1}$ **1b**	**1b** $\xrightarrow{k_3}$ **2**	**2** $\xrightarrow{k_5}$ **3**
^{13}C-KIE$^*_{C\text{-}1}$[a]			1.027
^{13}C-KIE$^*_{C\text{-}2}$[a]		1.041	
ϵ^*_C (‰)	−0.7	−10.1	−9.0
^{2}H-KIE$^*_{H\text{-}1}$[a]		0.925	
ϵ^*_H (‰)	−1.8	11.2	−18.0
$\Lambda^*_{H/C} = \epsilon^*_C/\epsilon^*_H$	2.6	−1.1	2.0

[a]Theoretical position-specific KIEs at C-1, C-2, or H-1 atom of nitrobenzene (see Section S7 for details).

KIEs at the reactive positions, C and H isotope enrichment factors (ϵ^*_C and ϵ^*_H), and $\Lambda^*_{H/C}$-values under the assumption that 1 of the 3 elementary reaction steps (i.e., **1a** → **1b**, **1b** → **2**, or **2** → **3**) was exclusively rate-limiting (see Section S7 for details). Theoretical nitrobenzene isotope fractionation during the oxygen activation step (**1a** → **1b**) was negligible compared to the subsequent oxygenation reactions. Our calculations show that ϵ^*_C-values for a rate-limiting step **1b** → **2** or **2** → **3** were similar (−10.1‰ and −9.0‰, respectively, Table 2) and much larger than experimental observations (−4.1 ± 0.2‰, Table 1). While theoretical H isotope fractionation was inverse for a rate-limiting step **1b** → **2**, it was normal for a rate-limiting step **2** → **3**. Experimental C and H isotope fractionation, however, can only be explained with the reactions shown in Scheme 1 with an overall normal theoretical H isotope fractionation. Therefore, the last step (**2** →**3**) must at least partly limit the rate of nitrobenzene dioxygenation. In fact, $\Lambda_{H/C}$ and $\Lambda^*_{H/C}$-values agreed very well (1.7 ± 0.5 vs 2.0, Table 1, entry 1, and Table 2). However, the fact that the theoretical ϵ^*_C for **2** → **3** was significantly larger than the experimental ϵ^{diox}_C-value also implies that a single rate-limiting step can not reconcile theory and experiment. Consequently, multiple elementary reactions were responsible for the observable isotope fractionation during nitrobenzene dioxygenation by NBDO.

We hypothesize that the experimental ^{13}C- and ^{2}H-AKIEs of the dioxygenation of nitrobenzene by NBDO (1.025 ± 0.001 and 1.027 ± 0.008, Table 1, entry 1) resulted from combined contributions of an O_2 activation step (**1a** → **1b**) and the second C−O bond formation step (**2** → **3**). From experimental AKIEs, which reflect the overall isotope effect of all elementary

DOI: 10.1021/acs.est.5b05084
Environ. Sci. Technol. 2016, 50, 6708−6716

reactions, and theoretical KIEs, we derived the commitment factors $(k_3/k_2)(k_5/k_4)$ and k_5/k_4 according to eq 5. The results are shown in Table S3. The commitment factors can be interpreted as the relative barrier heights, $\Delta G^{\ddagger}_{TS}$, pertinent to the transition states of the reactions displayed in Scheme 1.[28,29] The procedure is described in detail in the Section S7 and illustrated in Figure S4. The resulting range of the commitment factor k_5/k_4 was 0.12−0.52 (Table S3), which implies that the free energy of the transition state between species **2** and **3**, $\Delta G^{\ddagger}_{TS_{2/3}}$, was 2−5 kJ mol^{-1} higher than $\Delta G^{\ddagger}_{TS_{1b/2}}$ (i.e., the free energy of $TS_{1b/2}$). In addition, the range of $(k_3/k_2)(k_5/k_4)$ amounted to 1.6−2.5 (Table S3) and thus exceeded k_5/k_4 by a factor of 5−10. Consequently, the free energy of the $TS_{1a/1b}$ ($\Delta G^{\ddagger}_{TS_{1a/1b}}$) was approximately 2 kJ mol^{-1} higher than $\Delta G^{\ddagger}_{TS_{2/3}}$ and, thus, the barrier heights for the 3 reaction steps decreased in the order $\Delta G^{\ddagger}_{TS_{1a/1b}} > \Delta G^{\ddagger}_{TS_{2/3}} > \Delta G^{\ddagger}_{TS_{1b/2}}$. The commitment factors support the notion that the rate of nitrobenzene dioxygenation by NBDO was determined by the two elementary reactions **1a** → **1b** and **2** → **3**. As a consequence, the magnitude of the experimental ^{13}C- and ^{2}H-AKIEs for nitrobenzene was determined by contributions from the enzymatic O_2 activation *and* from bonding changes during the second C oxygenation.

The same reasoning can be applied to explain the variations of ^{13}C-AKIEs for the dioxygenation of the three nitrotoluene isomers by NBDO because the combined C and H isotope fractionation (i.e., $\Lambda_{H/C}$-values) suggested that the reaction mechanisms of the dioxygenation of nitrotoluenes and nitrobenzene were the same. ^{13}C-AKIE-values decrease from 1.018 ± 0.001 to 1.010 ± 0.001 in the order 2-nitrotoluene > 4-nitrotoluene ≈ 3-nitrotoluene (Figure 2c, Table 1, entries 2−4) indicating increasing contributions from O_2 activation. This interpretation is supported by the commitment factors shown in Table S3. In the case of 3-nitrotoluene dioxygenation by NBDO, O_2 activation may even be exclusively rate-limiting given that only negligible C isotope fractionation was observed. Note that we were not able to derive meaningful commitment factors for the dioxygenation of 2,6-dinitrotoluene by NBDO with the same mechanistic assumptions as for nitrobenzene and nitrotoluene isomers (Scheme 1, eq 5), which supports the interpretation of the larger $\Lambda_{H/C}$-values. The latter were taken as evidence for a different dioxygenation mechanism.

Kinetic Isotope Effects of NAC Dioxygenation by 2-Nitrotoluene Dioxygenase (2NTDO). We carried out a similar series of experiments with 2-nitrotoluene dioxygenase (2NTDO) to investigate whether the substrate dependence of dioxygenation KIEs, as seen for NBDO, also applies to other nitroarene dioxygenases. Isotopic enrichment factors for substrate disappearance (ϵ_C, ϵ_H) and dioxygenation (ϵ_C^{diox}), as well as γ_{diox}, $\Lambda_{H/C}$-, and AKIE-values, are compiled in Table 1 (entries 7−10). A detailed description of the reaction kinetics, product formation, and isotope fractionation in experiments with 2NTDO is provided in Section S9.

The relative proportions of substrate dioxygenation (γ_{diox}) by 2NTDO exceeded 93% and were, thus, larger than for NBDO, which is in agreement with previous studies.[21,22] This effect may be due to a bigger substrate pocket of 2NTDO for the accommodation of the CH_3-substituents.[58] Oxidation of the CH_3-group was only observed for 2- and 3-nitrotoluene (Table 1, entries 8 and 9). The sum of substrate and product concentrations in experiments with 3- and 4-nitrotoluene was below 70% of the initial substrate concentrations indicating an additional, so far unknown, pathway of substrate removal by 2NTDO. The formation of 2-methyl-5-nitrophenol from 4-nitrotoluene as well as two methylcatechol isomers from 3-nitrotoluene point toward a less regiospecific dioxygenation of nitrotoluenes by 2NTDO compared to NBDO.

C isotope fractionation for all four NACs with 2NTDO was always small; that is, the largest ϵ_C-values did not exceed −0.8 ± 0.2‰ and, therefore, did not reveal a notable substrate dependence. H isotope fractionation was also small but comparable to that observed with NBDO. The correlation of C and H isotope fractionation is illustrated in Figure 2b for the transformation of the three nitrotoluene isomers by 2NTDO. The trend lines as well as $\Lambda_{H/C}$-values were similar for 2- and 3-nitrotoluene suggesting again a common reaction mechanism. The same interpretation holds for 4-nitrotoluene but, due to the almost negligible C isotope fractionation, the $\Lambda_{H/C}$-value had a high uncertainty. As observed with NBDO, the $\Lambda_{H/C}$-value for nitrobenzene dioxygenation by 2NDTO was smaller than for the dioxygenation of nitrotoluene isomers by 2NTDO. The comparison of C vs H isotope fractionation for the four NACs and two nitroarene dioxygenases shows only minor differences and suggests that the mechanisms of dioxygenation, as shown in Scheme 1, were presumably the same with both enzymes. However, the uncertainties associated with $\Lambda_{H/C}$ are large due to the small C isotope fractionation measured for the four substrates.

The ^{13}C-AKIEs for the dioxygenation of nitrobenzene and 2-, 3-, and 4-nitrotoluene by 2NTDO shown in Figure 2c are substantially smaller than those measured with NBDO except for 3-nitrotoluene. On the basis of the reaction mechanism postulated above for the dioxygenation reactions with NBDO, we hypothesize that rates of NAC dioxygenation by 2NTDO were mainly determined by the initial O_2 activation step. It is likely that this elementary reaction of 2NTDO exhibited a similarly small isotope sensitivity like NBDO (**1a** → **1b**, Table 2) and, therefore, masked the contribution(s) of the C−O bond formation step(s) to the observable ^{13}C-AKIEs. From the very high dioxygenation yields of 2NTDO (γ_{diox}, Table 1), one may also speculate that 2NTDO catalyzed this reaction more efficiently than NBDO; that is, 2NTDO exhibits a higher commitment to catalysis.

IMPLICATIONS FOR CSIA OF AROMATIC CONTAMINANT BIODEGRADATION

The substrate-dependent C isotope fractionation during NAC dioxygenation illustrates some conceptual challenges associated with the quantitative assessment of biodegradation processes with CSIA. While a correlation of C, H, and N isotope fractionation may reveal the identity of the transformation pathway,[5,6] a quantification of the reaction progress implies reliable knowledge of the enrichment factors pertinent to the considered contaminant and transformation process. However, as shown here for the first time for oxygenations of aromatic compounds, isotope enrichment factors for a single contaminant and reaction can vary even within a family of structurally very similar enzymes (NBDO and 2NTDO share 95% of the amino acid residues in the subunit containing the active site).[21,23] For example, the extent of nitrobenzene dioxygenation associated with the minimum shift of δ^{13}C of ≥2‰, as recommended by Hunkeler et al.,[59] would correspond to 42% and 92% of fractional conversion, respectively, depending on whether the ϵ_C-values for NBDO and 2NTDO were used.

DOI: 10.1021/acs.est.5b05084
Environ. Sci. Technol. 2016, 50, 6708−6716

It is reasonable to assume that the kinetics of O_2 activating enzymes reported here may also affect the C isotope fractionation of the dioxygenation of other recalcitrant aromatic contaminants such as alkylated benzenes, polycyclic aromatic hydrocarbons, and chlorobenzenes by Rieske nonheme iron oxygenases.[60] In fact, the reported ^{13}C- and ^{2}H-AKIEs for those compounds are close to unity and in the same range as the numbers presented here for 2NTDO.[13−15,17] Our data suggest that further investigation on the mechanisms of aromatic carbon oxygenation as well as on the role of O_2 activation as a potentially rate-limiting reaction is warranted. This information could help to delineate cases where CSIA may be appropriate to track biological dioxygenations in contaminated soils and aquatic systems quantitatively from cases where it is not.

■ ASSOCIATED CONTENT

Supporting Information

The Supporting Information is available free of charge on the ACS Publications website at DOI: 10.1021/acs.est.5b05084.

Chemicals used, analyses, data evaluation procedures for product isotope signatures, theoretical position-specific isotope effects, derivation of commitment factors and theoretical ϵ and Λ-values, additional data, and figures illustrating kinetics and isotope fractionation of experiments with NBDO and 2NTDO. (PDF)

■ AUTHOR INFORMATION

Corresponding Author

*E-mail: thomas.hofstetter@eawag.ch; fax: +41 58 765 50 28; phone: +41 58 765 50 76.

Present Address

[‖]A.P.: Department of Cell and Molecular Biology, Uppsala University, Uppsala, Sweden.

Notes

The authors declare no competing financial interest.

■ ACKNOWLEDGMENTS

This work was supported by the Swiss-Polish Research Collaboration (PSRP-025/200 to T.B.H. and P.P.). We thank anonymous reviewers for their valuable comments.

■ REFERENCES

(1) Hofstetter, T. B.; Neumann, A.; Arnold, W. A.; Hartenbach, A. E.; Bolotin, J.; Cramer, C. J.; Schwarzenbach, R. P. Substituent effects on nitrogen isotope fractionation during abiotic reduction of nitroaromatic compounds. *Environ. Sci. Technol.* **2008**, *42*, 1997−2003.

(2) Hartenbach, A.; Hofstetter, T. B.; Berg, M.; Bolotin, J.; Schwarzenbach, R. P. Using nitrogen isotope fractionation to assess abiotic reduction of nitroaromatic compounds. *Environ. Sci. Technol.* **2006**, *40*, 7710−7716.

(3) Hartenbach, A. E.; Hofstetter, T. B.; Aeschbacher, M.; Sander, M.; Kim, D.; Strathmann, T. J.; Arnold, W. A.; Cramer, C. J.; Schwarzenbach, R. P. Variability of nitrogen isotope fractionation during the reduction of nitroaromatic compounds with dissolved reductants. *Environ. Sci. Technol.* **2008**, *42*, 8352−8359.

(4) Hofstetter, T. B.; Spain, J. C.; Nishino, S. F.; Bolotin, J.; Schwarzenbach, R. P. Identifying competing aerobic nitrobenzene biodegradation pathways using compound-specific isotope analysis. *Environ. Sci. Technol.* **2008**, *42*, 4764−4770.

(5) Wijker, R. S.; Bolotin, J.; Nishino, S. F.; Spain, J. C.; Hofstetter, T. B. Using compound-specific isotope analysis to assess biodegradation of nitroaromatic explosives in the subsurface. *Environ. Sci. Technol.* **2013**, *47*, 6872−6883.

(6) Wijker, R. S.; Kurt, Z.; Spain, J. C.; Bolotin, J.; Zeyer, J.; Hofstetter, T. B. Isotope fractionation associated with the biodegradation of 2-and 4-nitrophenols via monooxygenation pathways. *Environ. Sci. Technol.* **2013**, *47*, 14185−14193.

(7) Wijker, R. S.; Adamczyk, P.; Bolotin, J.; Paneth, P.; Hofstetter, T. B. Isotopic analysis of oxidative pollutant degradation pathways exhibiting large H isotope fractionation. *Environ. Sci. Technol.* **2013**, *47*, 13459−13468.

(8) Gorski, C. A.; Nurmi, J. T.; Tratnyek, P. G.; Hofstetter, T. B.; Scherer, M. M. Redox behavior of magnetite: Implications for contaminant reduction. *Environ. Sci. Technol.* **2010**, *44*, 55−60.

(9) Tobler, N. B.; Hofstetter, T. B.; Schwarzenbach, R. P. Assessing iron-mediated oxidation of toluene and reduction of nitroaromatic contaminants in anoxic environments using compound-specific isotope analysis. *Environ. Sci. Technol.* **2007**, *41*, 7773−7780.

(10) Spain, J. C.; Hughes, J. B.; Knackmuss, H. J. *Biodegradation of Nitroaromatic Compounds and Explosives*; Lewis Publishers: Boca Raton, FL, 2000.

(11) Ju, K.-S.; Parales, R. E. Nitroaromatic compounds, from synthesis to biodegradation. *Microbiol. Mol. Biol. Rev.* **2010**, *74*, 250−272.

(12) Eckert, D.; Qiu, S.; Elsner, M.; Cirpka, O. A. Model complexity needed for quantitative analysis of high resolution isotope and concentration data from a toluene-pulse experiment. *Environ. Sci. Technol.* **2013**, *47*, 6900−6907.

(13) Liang, X.; Howlett, M. R.; Nelson, J. L.; Grant, G.; Dworatzek, S.; Lacrampe-Couloume, G.; Zinder, S. H.; Edwards, E. A.; Lollar, B. S. Pathway-dependent isotope fractionation during aerobic and anaerobic degradation of monochlorobenzene and 1,2,4-trichlorobenzene. *Environ. Sci. Technol.* **2011**, *45*, 8321−8327.

(14) Morasch, B.; Richnow, H. H.; Schink, B.; Vieth, A.; Meckenstock, R. U. Carbon and hydrogen stable isotope fractionation during aerobic bacterial degradation of aromatic hydrocarbons. *Appl. Environ. Microbiol.* **2002**, *68*, 5191−5194.

(15) Fischer, A.; Herklotz, I.; Herrmann, S.; Thullner, M.; Weelink, S. A. B.; Stams, A. J. M.; Schloemann, M.; Richnow, H. H.; Vogt, C. Combined carbon and hydrogen isotope fractionation investigations for elucidating benzene biodegradation pathways. *Environ. Sci. Technol.* **2008**, *42*, 4356−4363.

(16) Fischer, A.; Gehre, M.; Breitfeld, J.; Richnow, H.-H.; Vogt, C. Carbon and hydrogen isotope fractionation of benzene during biodegradation under sulfate-reducing conditions: A laboratory to field site approach. *Rapid Commun. Mass Spectrom.* **2009**, *23*, 2439−2447.

(17) Dorer, C.; Vogt, C.; Kleinsteuber, S.; Stams, A. J.; Richnow, H.-H. Compound-specific isotope analysis as a tool to characterize biodegradation of ethylbenzene. *Environ. Sci. Technol.* **2014**, *48*, 9122−9132.

(18) Elsner, M. Stable isotope fractionation to investigate natural transformation mechanisms of organic contaminants: principles, prospects and limitations. *J. Environ. Monit.* **2010**, *12*, 2005−2031.

(19) Wijker, R. S.; Pati, S. G.; Zeyer, J.; Hofstetter, T. B. Enzyme kinetics of different types of flavin-dependent monooxygenases determine the observable contaminant stable isotope fractionation. *Environ. Sci. Technol. Lett.* **2015**, *2*, 329−334.

(20) Pati, S. G.; Kohler, H.-P. E.; Bolotin, J.; Parales, R. E.; Hofstetter, T. B. Isotope effects of enzymatic dioxygenation of nitrobenzene and 2-nitrotoluene by nitrobenzene dioxygenase. *Environ. Sci. Technol.* **2014**, *48*, 10750−10759.

(21) Lessner, D. J.; Johnson, G. R.; Parales, R. E.; Spain, J. C.; Gibson, D. T. Molecular characterization and substrate specificity of nitrobenzene dioxygenase from *Comamonas* sp. strain JS765. *Appl. Environ. Microbiol.* **2002**, *68*, 634−641.

(22) Parales, J. V.; Parales, R. E.; Resnick, S. M.; Gibson, D. T. Enzyme specificity of 2-nitrotoluene 2,3-dioxygenase from Pseudomonas sp. strain JS42 is determined by the C-terminal region of the alpha subunit of the oxygenase component. *J. Bacteriol.* **1998**, *180*, 1194−1199.

DOI: 10.1021/acs.est.5b05084
Environ. Sci. Technol. 2016, 50, 6708−6716

(23) Parales, J. V.; Kumar, A.; Parales, R. E.; Gibson, D. T. Cloning and sequencing of the genes encoding 2-nitrotoluene dioxygenase from Pseudomonas sp. JS42. *Gene* **1996**, *181*, 57−61.
(24) Ju, K.-S.; Parales, R. E. Control of substrate specificity by active-site residues in nitrobenzene dioxygenase. *Appl. Environ. Microbiol.* **2006**, *72*, 1817−1824.
(25) Lee, K.-S.; Parales, J.; Friemann, R.; Parales, R. Active site residues controlling substrate specificity in 2-nitrotoluene dioxygenase from Acidovorax sp. strain JS42. *J. Ind. Microbiol. Biotechnol.* **2005**, *32*, 465−473.
(26) Northrop, D. B. The expression of isotope effects on enzyme-catalyzed reactions. *Annu. Rev. Biochem.* **1981**, *50*, 103−131.
(27) Cleland, W. W. In *Isotope Effects in Chemistry and Biology*; Kohen, A., Limbach, H.-H., Eds.; CRC Press: Boca Raton, FL, 2006; Chapter 37 - Enzyme mechanisms from isotope effects, pp 915−930.
(28) Cook, P. F.; Cleland, W. W. *Enzyme Kinetics and Mechanism*; Garland Science Publishing Taylor & Francis Group: New York, USA, 2007.
(29) Purich, D. L. *Enzyme Kinetics: Catalysis & Control*; Elsevier Inc.: Amsterdam, 2010; Chapter 9 - Isotopic probes of biological catalysis, pp 575−636.
(30) Mahan, K. M. Structure function analysis of nitrobenzene 1,2-dioxygenase. Ph.D. thesis, University of California Davis, 2014.
(31) Lessner, D. J.; Parales, R. E.; Narayan, S.; Gibson, D. T. Expression of the nitroarene dioxygenase genes in *Comamonas* sp. Strain JS765 and *Acidovorax* sp. Strain JS42 Is induced by multiple aromatic compounds. *J. Bacteriol.* **2003**, *185*, 3895−3904.
(32) Haigler, B. E.; Wallace, W. H.; Spain, J. C. Biodegradation of 2-nitrotoluene by *Pseudomonas* sp. strain JS42. *Appl. Environ. Microbiol.* **1994**, *60*, 3466−3469.
(33) Parales, R. E.; Huang, R.; Yu, C.-L.; Parales, J. V.; Lee, F. K. N.; Lessner, D. J.; Ivkovic-Jensen, M. M.; Liu, W.; Friemann, R.; Ramaswamy, S.; Gibson, D. T. Purification, characterization, and crystallization of the components of the nitrobenzene and 2-nitrotoluene dioxygenase enzyme systems. *Appl. Environ. Microbiol.* **2005**, *71*, 3806−3814.
(34) An, D.; Gibson, D. T.; Spain, J. C. Oxidative release of nitrite from 2-nitrotoluene by a three-component enzyme system from *Pseudomonas* sp. strain JS42. *J. Bacteriol.* **1994**, *176*, 7462−7467.
(35) Berg, M.; Bolotin, J.; Hofstetter, T. B. Compound-specific nitrogen and carbon isotope analysis of nitroaromatic compounds in aqueous samples using solid-phase microextraction coupled to GC/IRMS. *Anal. Chem.* **2007**, *79*, 2386−93.
(36) Skarpeli-Liati, M.; Turgeon, A.; Garr, A. N.; Arnold, W. A.; Cramer, C. J.; Hofstetter, T. B. pH-Dependent equilibrium isotope fractionation associated with compound-specific nitrogen and carbon isotope analysis by SPME-GC/IRMS. *Anal. Chem.* **2011**, *83*, 1641−1648.
(37) Spahr, S.; Huntscha, S.; Bolotin, J.; Maier, M. P.; Elsner, M.; Hollender, J.; Hofstetter, T. B. Compound-specific isotope analysis of benzotriazole and its derivatives. *Anal. Bioanal. Chem.* **2013**, *405*, 2843−2856.
(38) Schimmelmann, A.; Lewan, M. D.; Wintsch, R. P. D/H isotope ratios of kerogen, bitumen, oil, and water in hydrous pyrolysis of source rocks containing kerogen types I, II, IIS, and III. *Geochim. Cosmochim. Acta* **1999**, *63*, 3751−3766.
(39) Schimmelmann, A.; Albertino, A.; Sauer, P. E.; Qi, H.; Molinie, R.; Mesnard, F. Nicotine, acetanilide and urea multi-level ^{2}H-, ^{13}C-and ^{15}N-abundance reference materials for continuous-flow isotope ratio mass spectrometry. *Rapid Commun. Mass Spectrom.* **2009**, *23*, 3513−3521.
(40) Godin, J. P.; McCullagh, J. S. O. Review: Current applications and challenges for liquid chromatography coupled to isotope ratio mass spectrometry (LC/IRMS). *Rapid Commun. Mass Spectrom.* **2011**, *25*, 3019−3028.
(41) Zhang, L.; Kujawinski, D. M.; Jochmann, M. A.; Schmidt, T. C. High-temperature reversed-phase liquid chromatography coupled to isotope ratio mass spectrometry. *Rapid Commun. Mass Spectrom.* **2011**, *25*, 2971−2980.
(42) Field, M. J.; Albe, M.; Bret, C.; Martin, P.-D.; Thomas, A. The dynamo library for molecular simulations using hybrid quantum mechanical and molecular mechanical potentials. *J. Comput. Chem.* **2000**, *21*, 1088−1100.
(43) Frisch, M. J. et al. *Gaussian 09, Revision A.02*; Gaussian, Inc.: Wallingford CT, 2009.
(44) Pabis, A.; Geronimo, I.; York, D. M.; Paneth, P. Molecular dynamics simulation of nitrobenzene dioxygenase using AMBER force field. *J. Chem. Theory Comput.* **2014**, *10*, 2246−2254.
(45) Pabis, A.; Geronimo, I.; Paneth, P. A DFT Study of the *cis*-dihydroxylation of nitroaromatic compounds catalyzed by nitrobenzene dioxygenase. *J. Phys. Chem. B* **2014**, *118*, 3245−3256.
(46) Hariharan, P. C.; Pople, J. A. The influence of polarization functions on molecular orbital hydrogenation energies. *Theor. Chimica Acta* **1973**, *28*, 213−222.
(47) Francl, M. M.; Pietro, W. J.; Hehre, W. J.; Binkley, J. S.; Gordon, M. S.; DeFrees, D. J.; Pople, J. A. Self-consistent molecular orbital methods. XXIII. A polarization-type basis set for second-row elements. *J. Chem. Phys.* **1982**, *77*, 3654−3665.
(48) Hay, P. J.; Wadt, W. R. Ab initio effective core potentials for molecular calculations. Potentials for K to Au including the outermost core orbitals. *J. Chem. Phys.* **1985**, *82*, 299−310.
(49) Scott, K. M.; Lu, X.; Cavanaugh, C. M.; Liu, J. S. Optimal methods for estimating kinetic isotope effects from different forms of the Rayleigh distillation equation. *Geochim. Cosmochim. Acta* **2004**, *68*, 433−442.
(50) Reichert, P. Aquasim - A tool for simulation and data-analysis of aquatic systems. *Water Sci. Technol.* **1994**, *30*, 21−30.
(51) Kovaleva, E. G.; Neibergall, M. B.; Chakrabarty, S.; Lipscomb, J. D. Finding intermediates in the O_2 activation pathways of non-heme iron oxygenases. *Acc. Chem. Res.* **2007**, *40*, 475−483.
(52) Kovaleva, E. G.; Lipscomb, J. D. Crystal structures of Fe^{2+} dioxygenase superoxo, alkylperoxo, and bound product intermediates. *Science* **2007**, *316*, 453−457.
(53) Kovaleva, E. G.; Lipscomb, J. D. Versatility of biological non-heme Fe (II) centers in oxygen activation reactions. *Nat. Chem. Biol.* **2008**, *4*, 186−193.
(54) Elsner, M.; Chartrand, M.; VanStone, N.; Lacrampe Couloume, G.; Sherwood Lollar, B. Identifying abiotic chlorinated ethene degradation: characteristic isotope patterns in reaction products with nanoscale zero-valent iron. *Environ. Sci. Technol.* **2008**, *42*, 5963−5970.
(55) Boyd, D. R.; Bugg, T. D. H. Arene *cis*-dihydrodiol formation: from biology to application. *Org. Biomol. Chem.* **2006**, *4*, 181−192.
(56) Bugg, T. D. Dioxygenase enzymes: catalytic mechanisms and chemical models. *Tetrahedron* **2003**, *59*, 7075−7101.
(57) Wolfe, M. D.; Parales, J. V.; Gibson, D. T.; Lipscomb, J. D. Single turnover chemistry and regulation of O_2 activation by the oxygenase component of naphthalene 1,2-dioxygenase. *J. Biol. Chem.* **2001**, *276*, 1945−1953.
(58) Friemann, R.; Ivkovic-Jensen, M. M.; Lessner, D. J.; Yu, C. L.; Gibson, D. T.; Parales, R. E.; Eklund, H.; Ramaswamy, S. Structural insight into the dioxygenation of nitroarene compounds: The crystal structure of nitrobenzene dioxygenase. *J. Mol. Biol.* **2005**, *348*, 1139−1151.
(59) Hunkeler, D.; Meckenstock, R.; Sherwood Lollar, B.; Schmidt, T. C.; Wilson, J. C. *A guide for assessing biodegradation and source identification of organic ground water contaminants using compound specific isotope analysis (CSIA)*; Office of Research and Development, US EPA: Washington, DC, 2008.
(60) Gibson, D. T.; Parales, R. E. Aromatic hydrocarbon dioxygenases in environmental biotechnology. *Curr. Opin. Biotechnol.* **2000**, *11*, 236−243.

DOI: 10.1021/acs.est.5b05084
Environ. Sci. Technol. 2016, 50, 6708−6716